Journal of Petroleum
Science and Technology

Prediction of Electrofacies Based on Flow Units Using NMR Data and SVM Method: a Case Study in Cheshmeh Khush Field, Southern Iran

Mahdi Rastegarnia[1], Mehdi Talebpour[2], Ali Sanati[3], and Seyed Hassan Hajiabadi[3]*

[1] Department of Petrophysics, Pars Petro Zagros Engineering and Services Company, Tehran, Iran
[2] Department of Petroleum Engineering, Islamic Azad University, Science and Research Branch, Tehran, Iran
[3] Faculty of Petrochemical and Petroleum Engineering, Hakim Sabzevari University, Sabzevar, Iran

ABSTRACT

The classification of well-log responses into separate flow units for generating local permeability models is often used to predict the spatial distribution of permeability in heterogeneous reservoirs. The present research can be divided into two parts; first, the nuclear magnetic resonance (NMR) log parameters are employed for developing a relationship between relaxation time and reservoir porosity as well as introducing the concept of relaxation group. This concept is then used for the definition of electrofacies in the studied reservoir. A graph-based clustering method, known as multi resolution graph-based clustering (MRGC), was employed to classify and obtain the optimum number of electrofacies. The results show that the samples with similar NMR relaxation characteristics were classified as similar groups. In the second part of the study, the capabilities of nonlinear support vector machine as an intelligent model is employed to predict the electrofacies and permeability distribution in the entire interval of the reservoir, where the NMR log parameters are unavailable. SVM prediction results were compared with laboratory core measurements, and permeability was calculated from stoneley wave analysis to verify the performance of the model. The predicted results are in good agreement with the measured parameters, which proves that SVM is a reliable tool for the identification of electrofacies through the conventional well log data.

Keywords: Flow Zone Index, Electrofacies, Support Vector Machine, Nuclear Magnetic Resonance, Conventional Petrophysical Data

INTRODUCTION

Geological and petrophysical properties play a significant role in fluid flow in the petroleum reservoirs. Hydraulic flow units are defined as correlatable and mappable zones within a reservoir which control fluid flow [1]. Flow units can be used to correlate important reservoir petrophysical parameters such as porosity and permeability and to facilitate field scale reservoir modeling tasks. Laboratory core measurement is the oldest techniques for obtaining porosity and permeability. Expensive costs and long times are the disadvantages of laboratory measurements. Meanwhile, it presents discontinuous information from subsurface formations. On the other hand, well logs can provide a continuous measurement of petrophysical characteristics of the subsurface

***Corresponding author**
Seyed Hassan Hajiabadi
Email: s.h.hajiabadi@hsu.ac.ir
Tel: +98 51 4401 2858
Fax: +98 51 4401 2851

Article history
Received: August 31, 2015
Received in revised form: November 25, 2015
Accepted: December 07, 2015
Available online: July 22, 2017

formations along the wellbore, and a wide range of geological characteristics of formations can be extracted from well log data. The present research aims to benefits from the advantage of well logs instead of expensive and time consuming core measurements. The identification of flow units through well log data is a cost-effective and potent method. As opposed to petrophysical parameters, lithology characterizations accompany with various challenges where a high degree of heterogeneity in rock formations is observed. In other words, the higher the heterogeneity of the reservoir is, the harder the predictions would be. Several researchers have identified flow units based on modeling workflows using the capabilities of intelligent models such as neural network (NN) models, principal component analysis (PCA), clustering methods, fuzzy logic (FL), hierarchical techniques, classification methods, and optimization algorithms [2-9]. Among various intelligent techniques, the present research selects support vector machines (SVM) to design a predictor model.

Studying previous literature shows that support vector machines (SVM) have demonstrated good generalization performance in many real-life applications [10-18]. This technique is a supervised machine learning algorithm based on the statistical learning theory developed by Vapnik [19]. SVM generates mapping functions from a set of labeled training data. On the other hand, SVM method is based on structural risk minimization principle, which in turn is based on the statistical learning theory. Statistical learning enhancement gives better generalization abilities by minimizing the testing error. SVM method can be used for nonlinear classification where kernel functions are used to map the input space into a higher-dimensional feature space. This effectively maps the non-linearity of the relationship to a linear one. SVM learning algorithm allows the sparse representation of models by considering only a portion of available training points which generate the support vectors [20]. Quadratic programming optimization is used to solve SVM formulation in dual space and nonlinear decision, and indicator hyper surfaces are then constructed in a functional form to classify new data and predict corresponding values [21]. SVM has been successfully used in a number of applications such as radar target detection [10], face detection [22], hand writing [11], text detection [13], speech recognition [14], financial time series prediction [15], porosity prediction [23], and lithology classification [16]; permeability reconstruction based on well log data [18], [23, 24] used SVM to estimate porosity using several well-log measurements, and it was demonstrated that SVM could be used instead of back-propagation neural network to predict permeability. For further details, the basic concepts of SVM are explained in the next section.

Nuclear magnetic resonance (NMR) log is one of the potent tools made a revolution in the measurement of reservoir properties which had been impossible to measure previously by logging instruments. Permeability and free and bulk fluid of rock, which was previously measured through time consuming laboratory measurements, can now be identified by NMR log without the necessity of expensive operation of coring.

In this research, the NMR responses are used to obtain an optimum number of electrofacies based on flow units. Data used in this study are related to Asmari reservoir in the Cheshmeh Khush oil field, Southern Iran (Figure 1). There are 3 wells, namely well A, B, and C. Well A has NMR and petrophysical evaluation results, and wells B and C have conventional data and petrophysical evaluation results. In wells B and C, permeability was calculated from stoneley wave analysis and core data.

The electrofacies modeling was first applied to well

A. Then, the defined electrofacies in well A were propagated in wells B and C by SVM method. For verifying these electrofacies, the results of SVM were compared with the results of petrophysical evaluation and core data as well as stoneley permeability in wells B and C; good agreement was achieved.

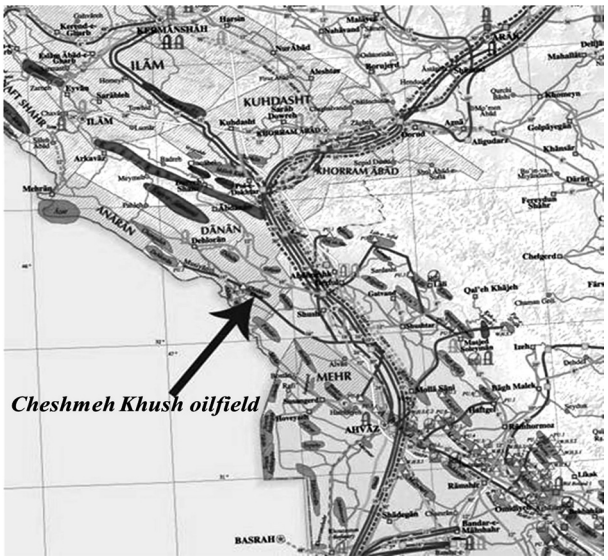

Figure 1: Location of the Cheshmeh Khush oilfield presented on the map.

EXPERIMENTAL PROCEUDRES

Support Vector Machine

SVM is a good procedure, which is able to deal with linear situations, always with the assumption that the data are separable without misclassifications by a linear hyper plane. The optimality criterion is to put the hyper plane as far as possible from the nearest samples, and keeping all the samples in their correct side. This means that maximum margin should be between the separating hyper plane and its nearest samples, and the margin hyper planes $w^T x + b = \pm 1$ must be placed into the separation margin; *w* is the optimum weight of the vector, and *x* and *b* are the bios of the model; *T* is the transpose notation. Consequently, SVM criterion is to maximize the distance between the separating hyper plane and the nearest samples subject to the constraints. The following equation describes the performance of SVM in a linear system (in the classification, it can be so called SVC)

$$L_D = -\frac{1}{2}\sum_{i=1}^{N}\sum_{j=1}^{N}\alpha_i\alpha_j y_i y_j x_i^{\mathrm{T}} x_j + \sum_{i=1}^{N}\alpha_i \quad (1)$$

where, *LD* is the notation of the basic equation of SVM in the linear system; α_i and α_i are the Lagrange multipliers; y_i and y_j are the binary scalar values; x_i and x_j are the input vector samples, and *N* is the number of samples.

Figure 2 shows the performance of SVM as a classifier in a linear system. The basic idea is that vectors *x* in a finite dimension space (called input space) can be mapped to a higher (possibly infinite) dimensional Hilbert space. A linear machine can be constructed in a higher dimensional space (often called the feature space), but it stays non-linear in the input space. Most of the transformations are unknown, but the dot product of the corresponding spaces can be expressed as a function of the input vectors as $\phi(x_i, x_j) = k(x_i, x_j)$. These spaces are called reproducing kernel Hilbert spaces (RKHS), and their dot products $k(x_i, x_j)$ are called Mercer kernels. The most common kernels, which are popular and used in many problems, are shown in the Table 1 [25].

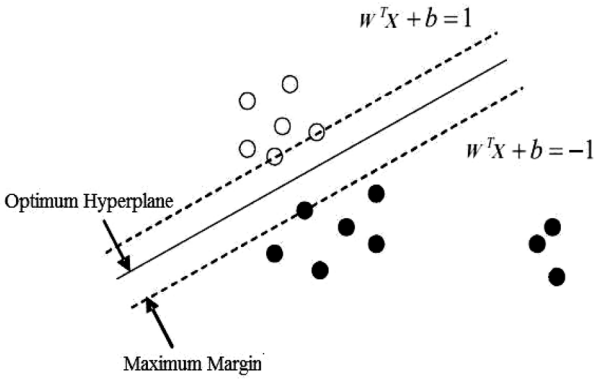

Figure 2: Performance of SVM in a linear system.

Table 1: Kernel and the type of classifier.

Kernel Function	Type of classifier
$K(x_i,x_j)=(x_i^{\mathrm{T}}x_j)^{\rho}$	Linear
$K(x_i,x_j)=(x_i^{\mathrm{T}}x_j+1)^{\rho}$	Complete polynomial of degree ρ
$K(x_i,x_j)=e^{\frac{\|x_i-x_j\|^2}{2\sigma^2}}$	Gaussian, radial basis function (RBF)
$K(x_i,x_j)=\tanh(\gamma x_i^{\mathrm{T}}x_j+\mu)$	Multilayer Perceptron
$K(\mathrm{x}_i,\mathrm{x}_j)=\frac{\sin\left[(n+1/2)(x_i-x_j)\right]}{2\sin[(\mathrm{x}_i-x_j)/2]}$	Dirichlet

Construction of a Nonlinear SVM

The solution for a linear SVM is indicated by a linear combination of the training data of $w=\sum_{i=1}^{N}y_i\alpha_i x_i$ to map the data into a Hilbert space, and then the solution is given by:

$$w=\sum_{i=1}^{N}y_i\alpha_i\varphi(x_i) \quad (2)$$

where, $\phi(x_i)$ is the mapping function. The parameter vector $\alpha_j < C$ is a combination of vectors into the Hilbert space, but many transformations $\phi(x_i)$ are unknown; however, the problem can still be solved because the machine just needs the dot products of the vector. We cannot use

$$y_i=w^{\mathrm{T}}\varphi(x_i)+b \quad (3)$$

since *w* parameters are in an infinite dimensional space; therefore, no expression exists for them. However, by substituting Equation 2 into Equation 1, the below equation is obtained.

$$y_i=\sum_{i=1}^{N}y_i\alpha_i\phi(x_i)^T\phi(x_j)+b=\sum_{i=1}^{N}y_i\alpha_i k(x_i,x_j)+b \quad (4)$$

The resulting machine can now be expressed directly in terms of the Lagrange multipliers and the kernel dot products. The kernel is used to compute this matrix $k_{ij}=k(x_i,x_j)$. When this matrix is computed, solving a non-linear SVM will be so easy. In order to compute the bias *b*, we can use $y_i(w^Tx_i+b)-1=0$, but for the nonlinear SVM, it changes to Equations 5 and 6.

$$y_i(\sum_{i=1}^{N}y_i\alpha_i\phi(x_i)^T\phi(x_j)+b)-1=0 \quad (5)$$

$$y_i(\sum_{i=1}^{N}y_i\alpha_i k(x_i,x_j)+b)-1=0 \quad (6)$$

for all x_j for which $\alpha_j < C$.

We just need to calculate *b* from the above expressions and calculate the mean value for all the samples with $\alpha_j < C$. The idea of a non-linear SVM can be seen in Figure 3.

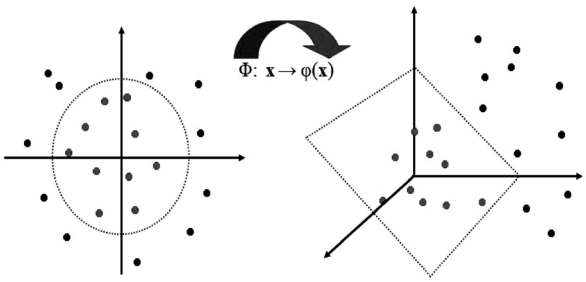

Figure 3: Original feature space can always be mapped to some higher-dimensional feature space by SVM.

Significance of NMR Logging in Reservoir Characterization

The importance and application of nuclear magnetic resonance (NMR) is not only limited to reservoir evaluation, but it is widely used in physics, chemistry, biology, and medicine. Combining the permanent magnets and pulsed radio frequencies with the concept of logging led to an important logging tool today known as NMR log in the world of petrophysicists. An applicable instrument of NMR logging was introduced by taking the benefits of a medicine magnetic resonance imaging (MRI) (6). This tool was the first NMR log that could be run into the formation rather that placing the rock sample in the instrument. Afterwards, several revisions were considered on his tool, and it was improved day by day; however, the

fundamental of all NMR logs is the same, where a magnetic field magnetized formation material using timed bursts of radio-frequency energy. The transmitted energy polarizes the spin axes of unaligned formation protons in a specific direction. By removing the transmitted magnetic field the protons start to align in their original direction. The time in which protons come back to their previous alignment is known as echo time. The amplitude of spin-echo trains are measured as a function of time, which is directly related to the number of hydrogen atoms of the fluid formation. Two time-based parameters of longitudinal relaxation time (T_1) and apparent relaxation time (T_2) are obtained from this step, and they include the most crucial outputs of NMR log leading to further properties of the formation. T_1 and T_2 indicate the time in which protons relax longitudinally and transversely respectively related to the transmitted magnetic field. In fact, T_2 is the most important parameter that can be directly converted to porosity. The T_2 plot includes movable and immovable fluids of the rock, which are separated based on a cut-off value of T_2. Only fluids are visible for transmitted magnetic field on NMR tool, and this fact redounds to one of the advantages of NMR log compared to conventional logs such as sonic, neutron, and bulk-density logs. In fact, the porosity measured by NMR log is not influenced from the matrix materials. In other words, NMR porosity is lithology-independent and does not need to be calibrated with lithology in different zones and intervals of a well. Three groups of invaluable information about reservoir condition can be obtained from NMR raw data, including pore size distribution of a formation, fluids properties of pore spaces, and finally quantities of these fluids. Porosity and pore size distribution are theoretically related to permeability in a direct relationship. Therefore, permeability and movable fluids (free fluid index) of the formation can be estimated using the aforementioned raw data. In the next section, the relation of T_2 and FZI is discussed.

Relation between NMR Log Responses and FZI

The fundamental equation which can relate the apparent relaxation rate of a single pore in the porous media is given by:

$$\frac{1}{T_2} = \frac{1}{T_{2b}} + \rho \frac{S}{V} \tag{7}$$

where, T_2 is the observed transverse relaxation time, and T_{2b} is the relaxation time of bulk fluid; ρ is relaxation surface, and S represents the surface area of the pore; V stands for the volume of the pore body. Since T_{2b} is significantly greater than the relaxation time (T_2) in the porous medium, the above equation can be reduced to:

$$\frac{1}{T} = \rho \frac{S}{V} \tag{8}$$

Georgi and Menger [26] proposed a relation between the surface area to volume ratio of the pore space, porosity, and the specific surface per grain volume ratio (S_{gv}). This relation was also used by Ohen et al. [27] and is given below:

$$\frac{S}{V} = S_{gv} \frac{1-\varphi}{\varphi} \tag{9}$$

Thus, Equation 7 can be written as:

$$\rho T_2 = \frac{\varphi}{[S_{gv}(1-\varphi)]} \tag{10}$$

or:

$$\frac{T_2}{\varphi_z} = \frac{1}{\rho S_{gv}} \tag{11}$$

Hence, Equations 10 and 11 can be related to *RQI* by:

$$RQI = \varphi_z .FZI = [\frac{\varphi}{1-\varphi}][\frac{1}{\tau S_{gv}\sqrt{F_s}}]$$

$$= \frac{\rho T_2}{(\tau\sqrt{F_s})} \tag{12}$$

This suggests that *RQI* is related to relaxation time and porosity group (ϕ_z). A logarithmic equation can be written using the above equations:

$$\log T_2 = \log(\varphi_z) + \log[\frac{1}{\rho S_{gv}}] \quad (13)$$

This equation relates relaxation time to porosity and forms the basis of relaxation group concept, which can be compared to the hydraulic unit concept. Equation 12 classifies samples which exhibit similar NMR relaxation (rock-fluid interaction) characteristics into a group. The average parameters for the group serve as calibration points for interpreting NMR logs. The factor $\frac{1}{\rho S_{gv}}$ is often recognized as relaxation product, and represents the relaxation power and textural attributes of the formation. As implied from Equation 13, the logarithmic plot of T_2 versus ϕ_z would result in a slope line, and $\frac{1}{\rho S_{gv}}$ would be constant for all data points on this slope line.

Formation rock samples or intervals with similar NMR relaxation characteristics lend themselves to the same group, with their $\log T_2$ versus $\log \phi_z$ clustering around the intercepting slope line. In this study, the samples or intervals of a formation or reservoir with similar NMR characteristics were considered in a similar relaxation group.

CASE STUDY

Methodology

Carbonate formations generally have wide pore size distributions, which ranges from microcrystalline pores to large vugs. Understanding the pore distribution and their geometries is vital for reservoir characterization. T_2 distributions are usually correlated with pore size and pore size distribution, so this fact is used for relating NMR responses to permeability. Micro, macro, and vuggy porosity are related to the NMR responses, which can be used to determine the effect of these types of porosities on permeability.

NMR responses are calibrated for predicting the irreducible bound fluid volume (BVI) using a variable T_2 cutoff, which can be derived from experimental measurements. By comparing the T_2 distributions of the fully saturated cores and the cores with irreducible saturation, a T_2 cutoff separating is obtained for the pore space, which participates in fluid migration from the non-participating pore space. The original method for computing permeability from NMR well logs using a fixed T_2 cutoff of 90 milli-seconds (ms) produces unreliable results in the carbonate formation. However, this method and the presence of isolated secondary porosities such as moldic and vuggy pores in carbonate could vary from 90 ms to 700 ms due to lithology heterogeneity and complex pore reservoirs. Therefore, several measurements are used to estimate the T_2 cut-off values for well log calibration in carbonates. Studying thin section, using scanning electron microscope (SEM) and computerized tomography (CT) image analysis along with the core data provides necessary information to evaluate T_2 cut-off method. Finally, this information can be employed to characterize vuggy carbonate lithology [28].

In this research, the spectral BVI (SBVI) method has been applied to determining permeability by using NMR data in well A. In this method, each pore size observed in the 100% brine-saturated spectra is assumed to contain some bound water. In this study, a two-step approach is proposed for electrofacies prediction from conventional logs data as explained below:

a) Determining optimum number of flow units using NMR data and MRGC method in well A.

b) Predicting electrofacies based on flow units from conventional logs using a support vector machine neural network (in wells B and C).

Multi Resolution Graph-based Clustering (MRGC)

Multi resolution graph-based clustering (MRGC) is a multi-dimensional dot-pattern recognition method based on non-parametric K-nearest-neighbor and graph data representation [29]. MRGC automatically determines the optimal number of clusters; also MRGC allows the geologist to control the level of detail actually needed to define the flow units. The underlying structure of the data is analyzed, and natural data groups are formed that may have very different densities, sizes, shapes, and relative separations. In this paper, the optimum number of flow units was found by MRGC method. The flow unit analysis was performed by clustering similar permeability, porosity, and volume T_2 distributions according to $\frac{1}{\rho S_{gv}}$.

Figure 4 shows the results obtained from MRGC clustering technique for limestone. Figure 4 presents the variations of relaxation time for each extracted flow unit.

Figure 5 shows the facies obtained after MRGC clustering method applied to the NMR data of well A. As shown, there is acceptable agreement among permeability log estimated by full wave sonic (PERM-ST), oil content, water saturation, and T_2, indicating the reliability of the technique used for clustering. Since the studied reservoir is a complex formation, clustering was separately used for both carbonate and sandstone lithological units. The variation of each parameter is shown in Figures 6 and 7.

Figure 8 displays the variation of grain size (T2LM) in carbonate and sandstone intervals. Facies No. 5 and No. 4 of carbonate intervals can be merged together as they have a suitable overlapping. This can also be considered for facies No. 5 and No. 6 of sandstone interval. Figure 9 shows the variation of grain size (T2LM) versus effective porosity in carbonate and sandstone intervals, where relaxation groups are distinguished.

	NAME	COL	PAT	WEIGHT	1/p.Sgv	MINIMUM	MAXIMUM	MEAN	STD DEV
1	FACIES_1			107		−0.01	0.06	0.01	0.02
2	FACIES_2			505		−0.99	−0.02	−0.34	0.29
3	FACIES_3			280		−1.64	−1.01	−1.34	0.18
4	FACIES_4			365		−2.47	−1.64	−2.05	0 24
5	FACIES_5			41		−2.56	−2.48	−2.52	0.02
6	FACIES_6			500		−4.29	−2.57	−3.02	0.31

Figure 4: Result of MRGC clustering in well A.

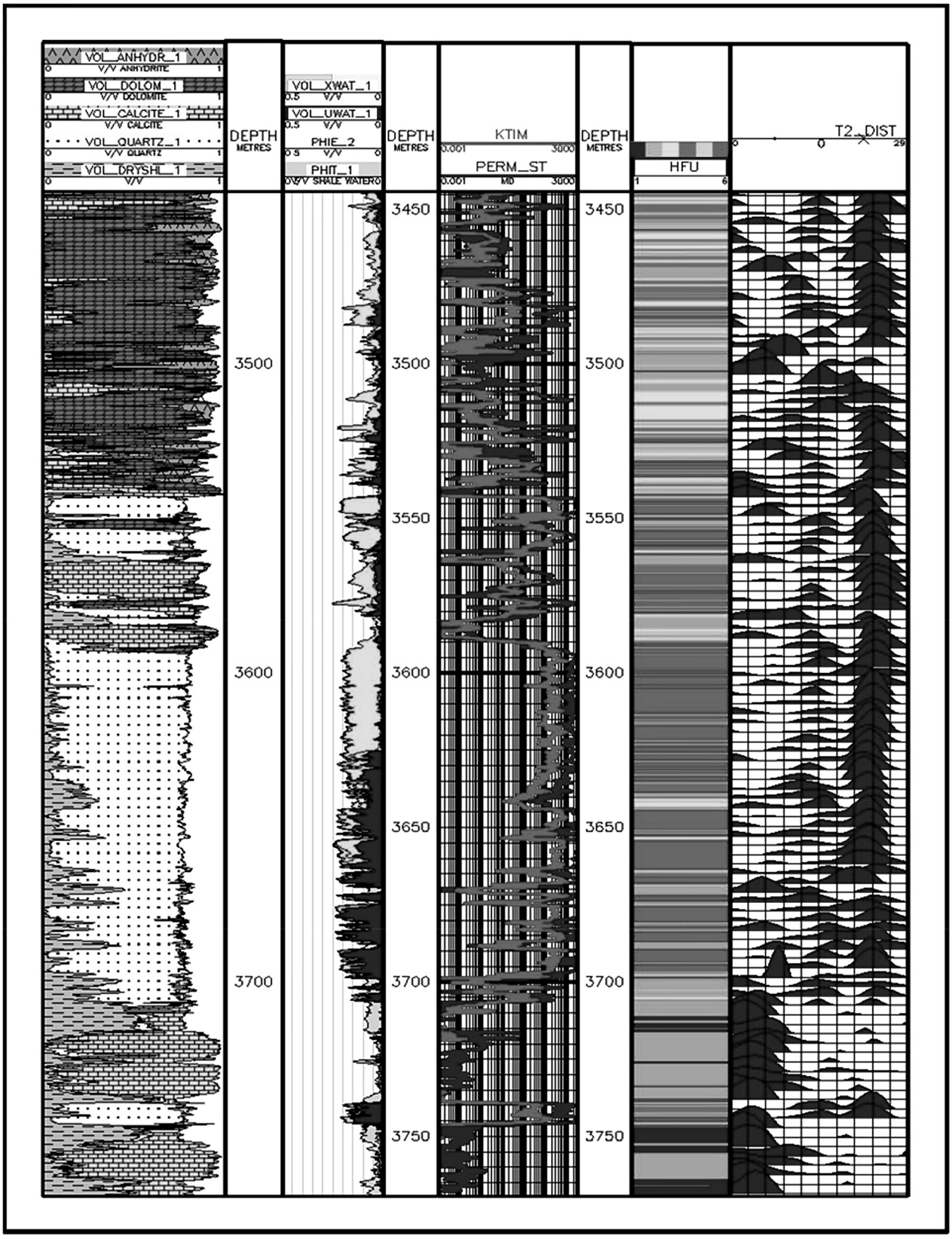

Figure 5: Facies obtained after applying MRGC clustering to well A.

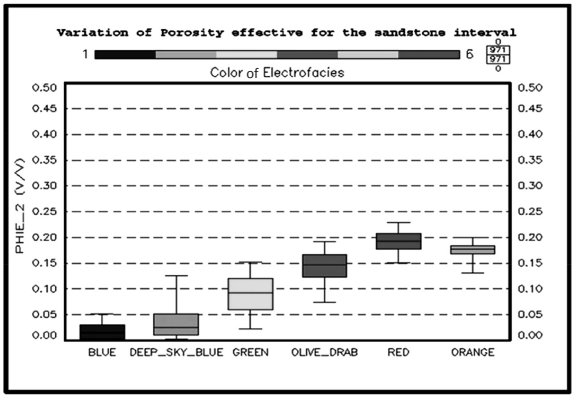

Figure 6A: Variation of effective Porosity for sandstone interval showing that facies No. 5 (Orange) and No. 6 (Red) can be merged together as they have a suitable overlapping.

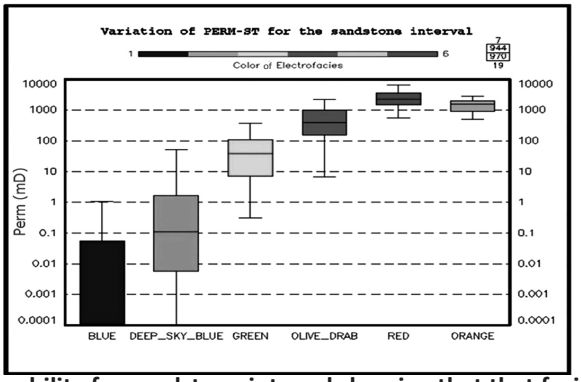

Figure 6B: Variation of permeability for sandstone interval showing that that facies No. 5 (Orange) and No. 6 (Red) have high permeability in value.

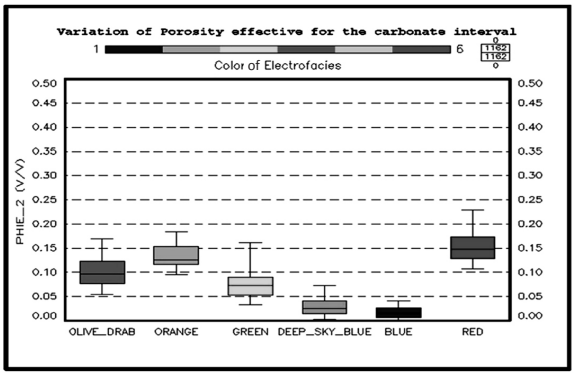

Figure 7A: Variation of effective Porosity for the carbonate interval showing that facies No. 5 (Orange) and No. 4 (Olive_Darb) can be merged together as they have a suitable overlapping.

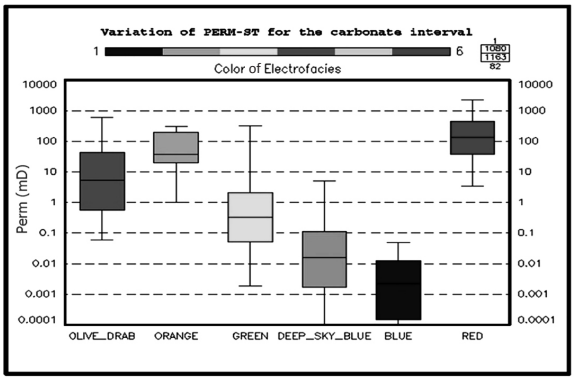

Figure 7B: Variation of permeability for the carbonate interval showing that facies No. 5 (Orange) and No. 4 (Olive_ Darb) have high permeability in value.

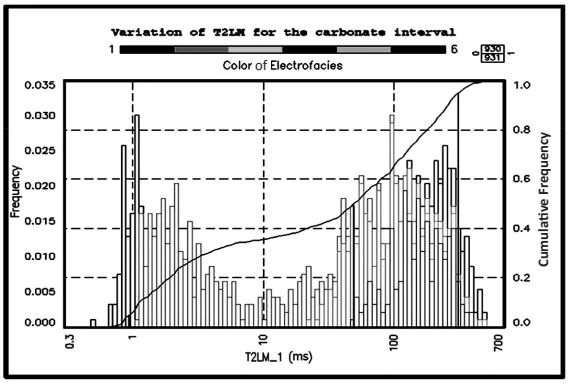

Figure 8A: Variation of grain size (T2LM) for the carbonate interval showing that facies No. 5 (Orange) and No. 4 (Olive_Darb) have a suitable overlapping.

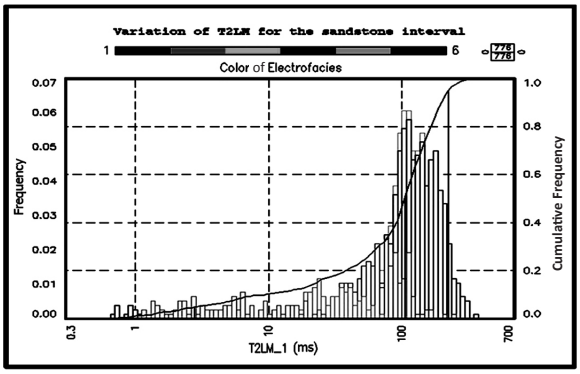

Figure 8B: Variation of grain size for the sandstone showing that facies No. 5 (Orange) and No. 6 (Red) have a suitable overlapping.

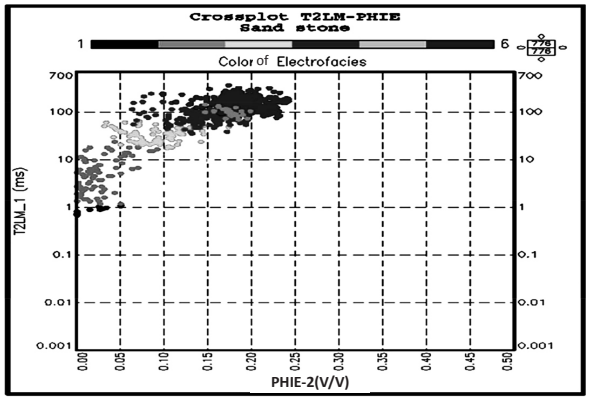

Figure 9A: Cross plot of MRGC clustering results of NMR log measurements to identify facies for sandstone interval.

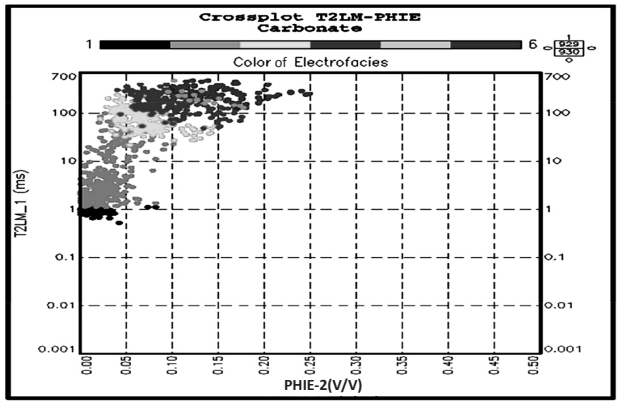

Figure 9B: Cross plot of MRGC clustering results of NMR log measurements to identify facies for carbonate interval.

Prediction of Electrofacies Using Support Vector Machine

In this step, those facies obtained during clustering by MRGC were taken into consideration to be predicted by support vector machine (SVM). Since the background of SVM has been extensively presented in the literature, we brought the background in the Appendix section. To run the SVM for this prediction, two separate models were built for the sandstone and carbonate intervals. For this purpose, porosity log (PHIE), total porosity (PHIT), and DT logs were considered as the inputs to carbonate intervals whereas porosity log (PHIE), total Porosity log (PHIT), DT log, and RHOB log were taken as the inputs for the estimation of electrofacies in sandstone intervals. Available data were normalized to be in the range of 0 and 1. A trial and error method was used to determine the parameters of the SVM, including parameters C and kernel type. Table 2 tabulates the optimum value of the SVM parameters determined during the trial and error methods. Tables 3 and 4 respectively list the confusion matrix showing the results of prediction using the SVM method.

Table 2: Parameters of SVM determined using a trial and error method.

Type reservoir	Kernel	C	Accuracy
Sand stone	Gaussian	50	83.62%
Carbonate	Gaussian	3200	78.81%

Table 3: Confusing matrix of carbonate interval showing the prediction results obtained by SVM.

Carbonate						
	Predicted					
Actual		Electrofacies 1	Electrofacies 2	Electrofacies 3	Electrofacies 4	Electrofacies 5
	Electrofacies 1	8	6	0	0	0
	Electrofacies 2	2	51	3	2	0
	Electrofacies 3	0	3	21	6	1
	Electrofacies 4	0	0	4	24	1
	Electrofacies 5	0	0	0	4	15

Table 4: Confusing matrix of sandstone interval showing the prediction results obtained by SVM.

Sand stone						
	Predicted					
Actual		Electrofacies 1	Electrofacies 2	Electrofacies 3	Electrofacies 4	Electrofacies 5
	Electrofacies 1	1	1	0	0	0
	Electrofacies 2	0	11	3	0	0
	Electrofacies 3	0	1	8	3	0
	Electrofacies 4	0	0	2	16	4
	Electrofacies 5	0	0	0	5	61

In addition, the accuracy and recall values of each electrofacies predicted by SVM were calculated and are presented in Tables 5 and 6.

After achieving the suitable results during the training and testing of SVM in the prediction of electrofacies, the SVM was used to predict the electrofacies of wells B and C. Figures 10 and 11 show the results of SVM prediction in wells B and C. The results of prediction in wells B and C were calibrated using the results obtained using core and full wave sonic data as well as petrophysical evaluation. The results show acceptable agreements between the results of SVM prediction and those of the petrophysical evaluations.

Table 5: Accuracy and recall values of each electrofacies in the carbonate interval predicted by SVM.

Carbonate	Electrofacies 1	Electrofacies 2	Electrofacies 3	Electrofacies 4	Electrofacies 5
Precision	0.8	0.85	0.75	0.667	0.882
Recall	0.57	0.864	0.677	0.827	0.789

Table 6: Accuracy and recall values of each electrofacies in the sandstone interval predicted by SVM.

Sand stone	Electrofacies 1	Electrofacies 2	Electrofacies 3	Electrofacies 4	Electrofacies 5
Precision	1	0.846	0.615	0.667	0.8938
Recall	0.5	0.786	0.667	0.727	0.924

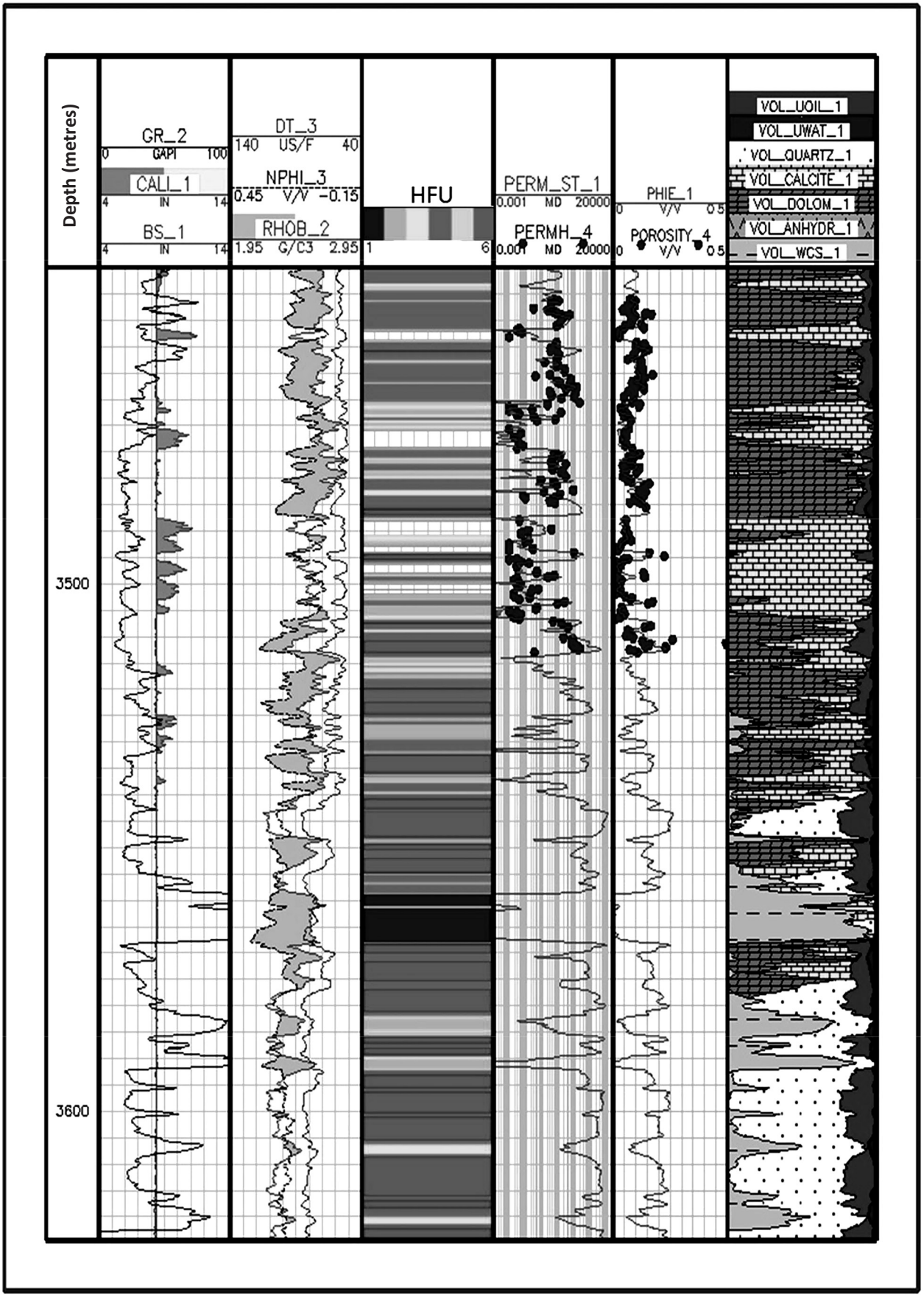

Figure 10: Electrofacies predicted by SVM in well B.

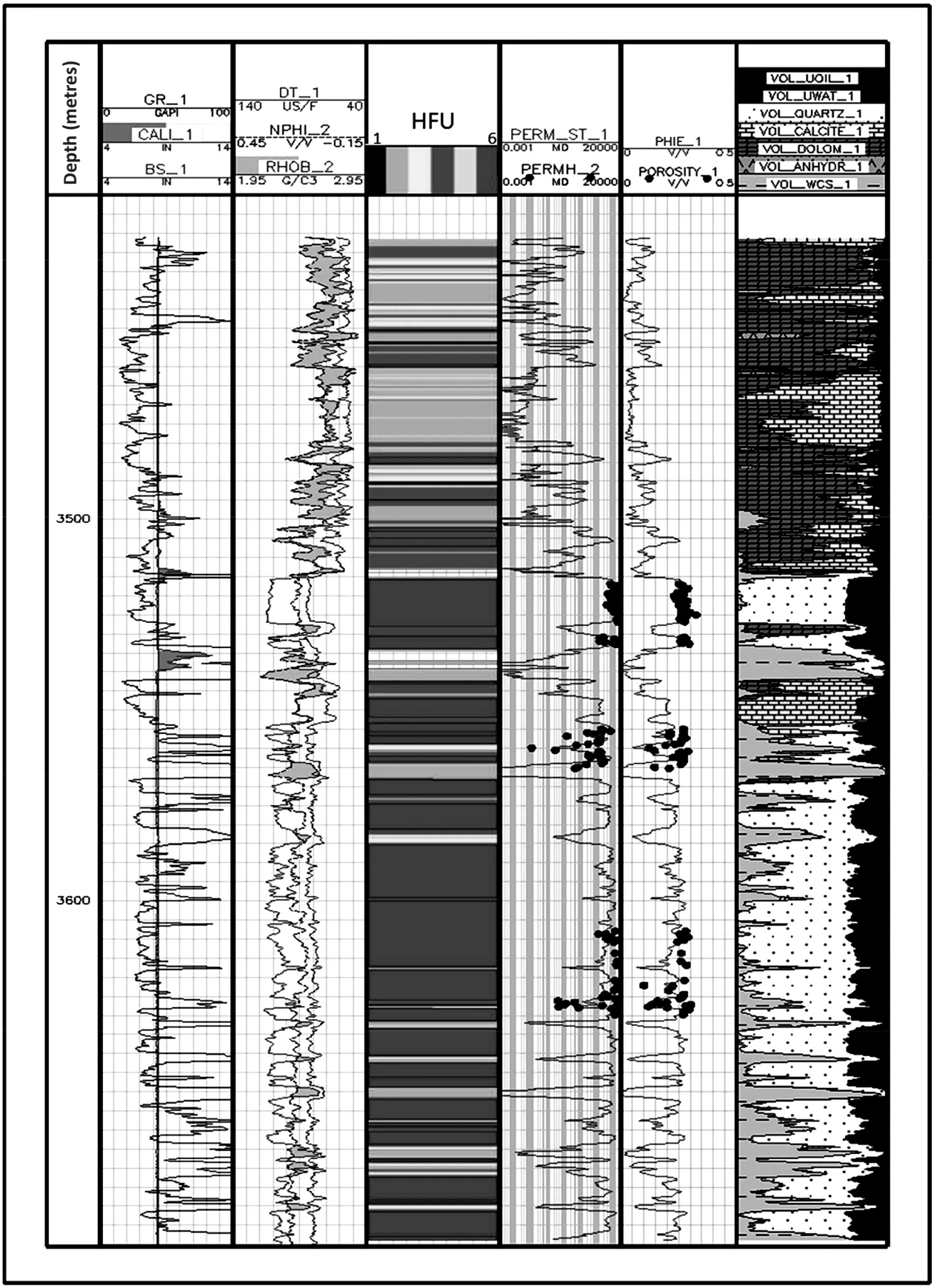

Figure 11: Electrofacies predicted by SVM in well C.

CONCLUSIONS

In this paper, the application of two robust methods, namely multi-resolution graph-based clustering (MRGC) and support vector machine (SVM), was proven through utilizing the well data of a reservoir located in the south of Iran. MRGC technique was used for clustering the electrofacies carbonate and sandstone intervals. SVM was then utilized to predict the electrofacies determined by the MRGC technique. Porosity, sonic, and density logs were considered as the input to the prediction of electrofacies, and the results have proved to be valid since there was a good match between the prediction results of SVM and those of petrophysical evaluation.

ACKNOWLEDGEMENTS

Special thanks are given to Iranian Central Oil Company for providing us with the data and cooperation.

REFERENCES

1. Tiab D. and Donaldson E. C., "Petrophysics Theory and Practice of Measuring Reservoir Rock and Fluid Transport Properties," *Elsevier Press*, Oxford, **2004**, 112-132.
2. Busch J., Fortney W., and Berry L., "Determination of Lithology from Well Logs by Statistical Analysis," *SPE Formation Evaluation*, **1987**, *2*(04), 412-418.
3. Delfiner P., Peyret O., and Serra O., "Automatic Determination of Lithology from Well Logs," *SPE Formation Evaluation*, **1987**, *2*(03), 303-310.
4. El-Sheikh T. S. and Syiam M., "An Efficient Technique for Lithology Classification," *Geoscience and Remote Sensing*, **1989**, *27*(5), 629-632.
5. Lim J. S., Kang J. M., and Kim J., "Multivariate Statistical Analysis for Automatic Electrofacies Determination from Well log Measurements," in *Asia Pacific Oil & Gas Conference & Exhibition,* **1997.**
6. Huang T. M., Kecman V., and Kopriva I., "Kernel Based Algorithms for Mining Huge Data Sets," *Springer*, **2006**, *17*, 125-173.
7. Chikhi S. and Shout H., "Using Probabilistic Neural Networks to Construct Well Facies," *WSEAS Trans. Syst*., **2003**, *2*(4), 839-843.
8. Chikhi S., Batouche M., and Shout H., "Hybrid neural Network Methods for Lithology Identification in the Algerian Sahara," *International Journal of Computational Intelligence*, **2005**, *1*(1), 25-33.
9. Carrasquilla A., Silvab J., and Flexa R., "Associating Fuzzy Logic, Neural Networks and Multivariable Statistic Methodologies in the Automatic Identification of Oil Reservoir Lithologies through Well Logs," *Revista de Geologia*, **2008**, *21*(1), 27-34.
10. Li Z., Weida Z., and Licheng J., "Radar Target Recognition Based on Support Vector Machine," in Signal Processing Proceedings, WCCC-ICSP, 5th International Conference on. 2000. IEEE, **2000**.
11. Choisy C. and Belaid A., "Handwriting Recognition Using Local Methods for Normalization and Global Methods for Recognition in Document Analysis and Recognition," Proceedings. 6th International Conference on. 2000. IEEE, **2001**.
12. Gao J., Harris C. J., and Gunn S. R., "On a Class of Support Vector Kernels Based on Frames in Function Hilbert Spaces," *Neural Computation*, **2001**, *13*(9), 1975-1994.
13. Shin C., Kim K. I., Park M. H., and Kim H. J., "Support Vector Machine-based Text Detection in Digital Video," in *Neural Networks for Signal Processing X*, Proceedings of the 2000 IEEE Signal Processing Society Workshop, **2000**.
14. Ma C., Randolph M. A., and Drish J., "A Support Vector Machines-based Rejection Technique for Speech Recognition," in *Acoustics, Speech, and*

Signal Processing, Proceedings.(ICASSP›01). 2001 IEEE International Conference on. 2001. IEEE, **2001**.

15. Van Gestel T., Suykens J. A. K., Baestaens D. E., Lambrechts A., et al., "Financial Time Series Prediction using Least Squares Support Vector Machines within the Evidence Framework," *Neural Networks*, IEEE Transactions on, **2001**, *12*(4), 809-821.
16. Al-Anazi A. and Gates I., "On the Capability of Support Vector Machines to Classify Lithology from Well Logs," *Natural Resources Research*, **2010**, *19*(2), 125-139.
17. Al-anazi A. F. and Gates I. D., "Support-vector regression for permeability prediction in a heterogeneous reservoir: A comparative study," *SPE Reservoir Evaluation & Engineering*, **2010**, *6*(10), 21-18.
18. Al-Anazi A. and Gates I., "Support Vector Regression for Porosity Prediction in a Heterogeneous Reservoir: A Comparative Study," *Computers & Geosciences*, **2010**, *36*(12), 1494-1503.
19. Vapnik V., "The Nature of Statistical Learning Theory," Springer Science & Business Media, **2000**.
20. Wang L., "Support Vector Machines: Theory and Applications," Springer Science & Business Media, **2005**:
21. Al-Anazi A., Gates I., and Azaiez J., "Fuzzy Logic Data-driven Permeability Prediction for Heterogeneous Reservoirs," Paper SPE 121159 Presented at *the EUROPEC/EAGE Conference and Exhibition*, **2009**.
22. Lu J., Plataniotis K., and Ventesanopoulos A., Face Recognition Using Feature Optimization and V-support Vector Machine," *IEEE Neural Netw. Signal Process*, **2001**, 373–382.
23. Wong K.W.,Fung C. C., Ong Y. S., and Gedeon T. D., "Reservoir Characterization Using Support Vector Machines," in Computational Intelligence for Modelling, Control and Automation, 2005 and International Conference on Intelligent Agents, Web Technologies and Internet Commerce, International Conference on. 2005. IEEE., **2005**.
24. Al-Anazi A. and Gates I., "Support Vector Regression to Predict Porosity and Permeability: Effect of Sample Size," *Computers & Geosciences*, **2012**, *39*, 64-76.
25. Suykens J. A., "Data Visualization and Dimensionality Reduction Using Kernel Maps with a Reference Point," *Neural Networks*, *IEEE Transactions*, **2008**, *19*(9), 1501-1517.
26. Georgi D. and Menger S., "Reservoir Quality, Porosity and Permeability Relationships," *in Proc. 14th Mintrop Seminar*, Münster. **1994**.
27. Ohen H. A. and Ajufo A., "A Hydraulic (Flow) UMR Based Model for the Determination of Petrophysical Properties from nmr Relaxation Measurements," SPE Annual Technical Conference and Exhibition, Dallas, Texas, **1995**.
28. Parra J., Hackert C. L., Collier H. A., and Bennett M., "NMR and Acoustic Signatures in Vuggy Carbonate Aquifers," in SPWLA 42nd Annual Logging Symposium, Society of Petrophysicists and Well-Log Analysts, **2001**.
29. Ye S. J. and Rabiller P., "A New Tool for Electro-Facies Analysis: Multi-resolution Graph-based Clustering," in SPWLA 41st annual logging symposium, Society of Petrophysicists and Well-Log Analysts, **2000**.